Please cite this article in press as: Viney et al., Local Retinal Circuits of Melanopsin- Containing Ganglion Cells Identified by Transsynaptic Viral Tracing, Current Biology (2007), doi:10.1016/j.cub.2007.04.058

Current Biology *17*, 1–8, June 5, 2007 ©2007 Elsevier Ltd All rights reserved DOI 10.1016/j.cub.2007.04.058

Report

Local Retinal Circuits of Melanopsin-Containing Ganglion Cells Identified by Transsynaptic Viral Tracing

Tim James Viney,[1] Kamill Balint,[1,7] Daniel Hillier,[1,3] Sandra Siegert,[1] Zsolt Boldogkoi,[7] Lynn W. Enquist,[4] Markus Meister,[5] Constance L. Cepko,[6] and Botond Roska[1,2,5,6,*]

[1] Neural Circuit Laboratories
Friedrich Miescher Institute
Maulbeerstrasse 66
Basel 4058
Switzerland

[2] Harvard Society of Fellows
Harvard University
78 Mount Auburn Street
Cambridge, Massachusetts 02138

[3] Department of Information Technology
Pazmany Peter Catholic University
Prater utca 50/a
Budapest 1083
Hungary

[4] Department of Molecular Biology
Princeton University
314 Schultz Laboratory
Washington Road
Princeton, New Jersey 08544

[5] Department of Molecular and Cellular Biology
Harvard University
7 Divinity Avenue
Cambridge, Massachusetts 02138

[6] Department of Genetics
Harvard Medical School
77 Avenue Louis Pasteur
Boston, Massachusetts 02115

[7] Department of Biology
Faculty of Medicine
University of Szeged
H-6720 Szeged
Hungary

Summary

Intrinsically photosensitive melanopsin-containing retinal ganglion cells (ipRGCs) control important physiological processes, including the circadian rhythm, the pupillary reflex, and the suppression of locomotor behavior (reviewed in [1]). ipRGCs are also activated by classical photoreceptors, the rods and cones, through local retinal circuits [2, 3]. ipRGCs can be transsynaptically labeled through the pupillary-reflex circuit with the derivatives of the Bartha strain of the alphaherpesvirus pseudorabies virus(PRV) [4, 5] that express GFP [6–12]. Bartha-strain derivatives spread only in the retrograde direction [13]. There is evidence that infected cells function normally for a while during GFP expression [7]. Here we combine transsynaptic PRV labeling, two-photon laser microscopy, and electrophysiological techniques to trace the local circuit of different ipRGC subtypes in the mouse retina and record light-evoked activity from the transsynaptically labeled ganglion cells. First, we show that ipRGCs are connected by monostratified amacrine cells that provide strong inhibition from classical-photoreceptor-driven circuits. Second, we show evidence that dopaminergic interplexiform cells are synaptically connected to ipRGCs. The latter finding provides a circuitry link between light–dark adaptation and ipRGC function.

Results and Discussion

PRV152 Labels Morphologically Distinct Retinal-Ganglion-Cell Subtypes

To transneuronally label intrinsically photosensitive melanopsin-containing retinal ganglion cells (ipRGCs) via the autonomic circuits, we injected PRV152 into the anterior chamber (AntC) of the right eye of mice (Figure 1A) [4, 13, 14]. After 3.5–4.5 days, we isolated the retina from the left eye (n = 36 retinas), where several ganglion cells were brightly labeled with GFP (Figure 1B).

Dendrites of mouse retinal ganglion cells of different morphological and physiological classes [15–17] ramify at different depths (strata) in the inner plexiform layer (IPL) [18, 19]. All of 170 analyzed GFP-expressing ganglion cells in the left retina were found to have dendrites in only two IPL strata at depths of 30% (±4%) and 89% (±6%). These dendritic strata were outside the two outer strata labeled by the calretinin antibody (Figures 1C and 1D) [20] and in the same strata specifically labeled by the melanopsin antibody (Figures 1C and 1D). In the brain, similar retinorecipient nuclei were labeled bilaterally (Figure 1E) as described in hamsters and rats [13, 21], including the suprachiasmatic nucleus (SCN), the intergeniculate leaflet (IGL), and the olivary pretectal nucleus (OPN). The dorsal lateral geniculate nucleus (dLGN) and the superior colliculus (SC) were not labeled, even at 5 days after infection (Figure 1E). Ganglion cells in other retinal strata can be labeled from the superior colliculus and the primary visual cortex (V1), ruling out the possibility that only certain subtypes of ganglion cells have receptors for pseudorabies virus (PRV) (Figure S1A in the Supplemental Data available online). These experiments suggest that contralateral PRV152 infection into the AntC labels subclasses of mouse ganglion cells that project to the SCN, the IGL, and the OPN, which are known targets of melanopsin-expressing ganglion cells [22, 23].

Three and a half to four days after virus infection, 99% (79/80 cells counted from two infected retinas) of the labeled cells were melanopsin positive, whereas the fraction among all ganglion cells is estimated at 1%–2% [24, 25], suggesting that during the first wave of infection, almost all labeled ganglion cells are ipRGCs. However, around 5 days after virus infection, only 50% of the GFP-expressing ganglion cells were positive for melanopsin

*Correspondence: botond.roska@fmi.ch

Please cite this article in press as: Viney et al., Local Retinal Circuits of Melanopsin- Containing Ganglion Cells Identified by Transsynaptic Viral Tracing, Current Biology (2007), doi:10.1016/j.cub.2007.04.058

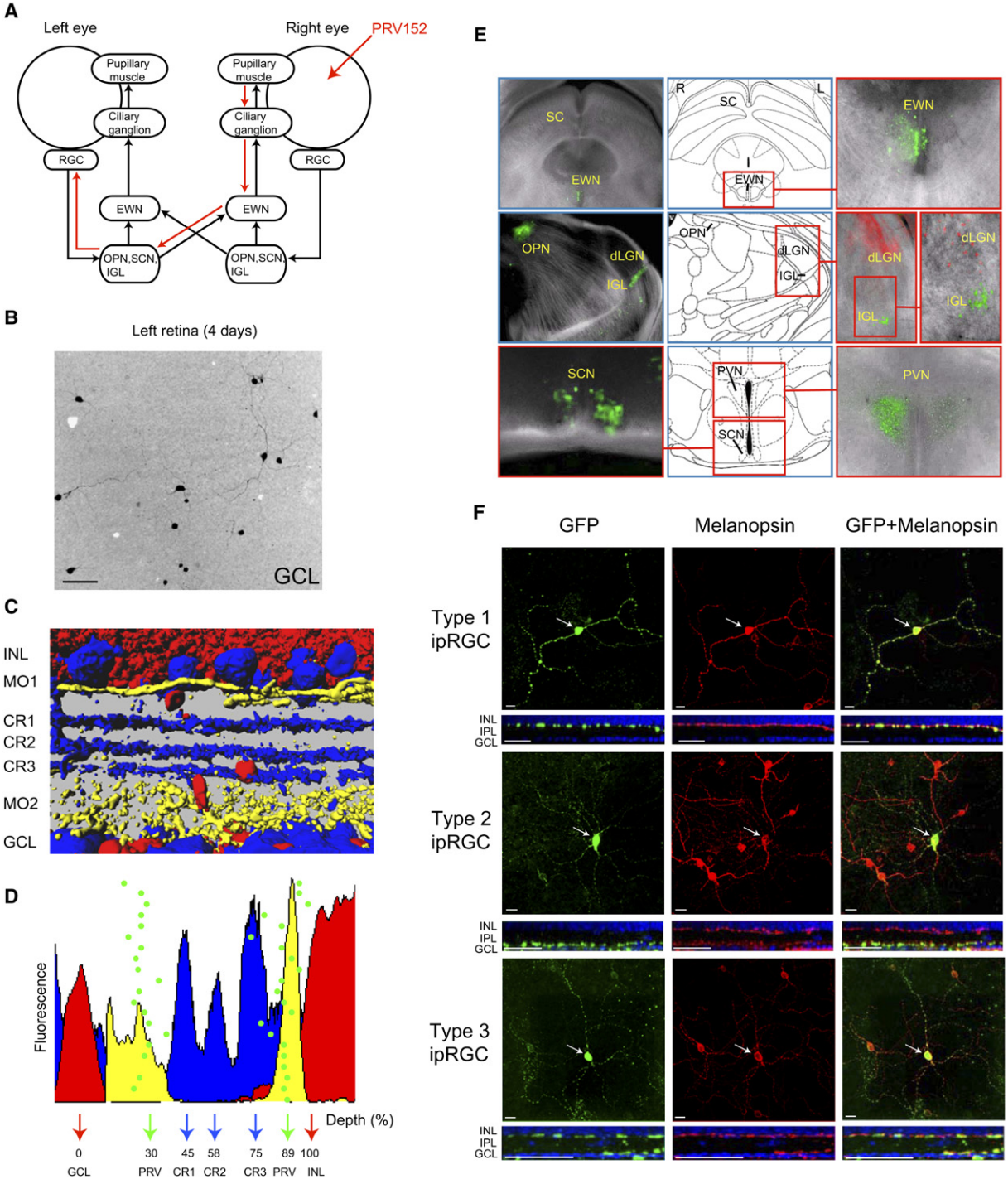

Figure 1. PRV152 Retrogradely Spreads from the Right Eye to Subtypes of Ganglion Cells in the Left Retina

(A) Simplified schematic of the PRV spread [7, 13]. Red arrows indicate the route of retrograde virus spread from the right eye to the contralateral retinal ganglion cells (RGCs).

(B) Low-resolution (10×) confocal scan of the left retina 4 days after injection, showing several GFP-labeled ganglion cells. The scale bar represents 100 μm.

(C) Confocal reconstruction from a 200-μm-thick vibratome section. Calretinin antibody (blue) labels three strata in the IPL (CR1, CR2, and CR3). Cell nuclei are labeled with DAPI (red). Melanopsin antibody (yellow) labels two strata (MO1 and MO2).

(D) The depths of dendritic ramification of PRV152-labeled ganglion cells are plotted as green dots. Monostratified cells are presented as one dot; bistratified ganglion cells are presented as two dots. The fluorescence as a function of depth is plotted for calretinin (blue), DAPI (red), and melanopsin (yellow). The x axis shows the relative depth in the IPL; the y axis shows normalized fluorescence.

(E) Brain regions labeled 5 days after injection of PRV152 into the anterior chamber (AntC) of the right (R) eye and PRV614 (RFP-expressing variant) to the left (L) visual cortex. PRV152 (green) labels the EWN, OPN, IGL, SCN, and hypothalamic paraventricular nucleus (PVN) but not the SC or the dLGN. PRV614 (red) labels the dLGN. Diagrams are taken from [43].

Please cite this article in press as: Viney et al., Local Retinal Circuits of Melanopsin- Containing Ganglion Cells Identified by Transsynaptic Viral Tracing, Current Biology (2007), doi:10.1016/j.cub.2007.04.058

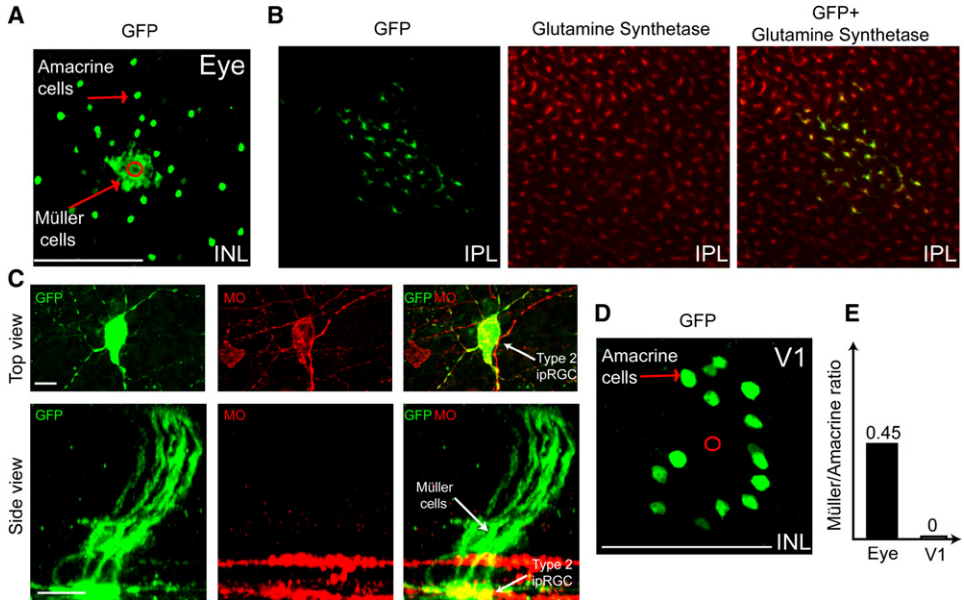

Figure 2. GFP-Labeled Local Circuits 5 Days after PRV152 Injection into the AntC of the Right Eye or the Right V1 Cortical Region

(A) GFP-positive amacrine and Müller cells in the INL. The red circle indicates the position of the GFP-positive ganglion cell in the GCL. The scale bar represents 100 μm.

(B) Colocalization of the Müller-cell marker glutamine synthetase (red) and GFP (green) for cells that are centrally GFP labeled near a GFP-positive ganglion cell. The depth of the scan is in the middle of the IPL.

(C) Top views of a GFP-labeled type 2 ipRGC with corresponding side views of labeled Müller cells. GFP (green) colocalizes with melanopsin (MO, red). The scale bar represents 15 μm.

(D) A confocal scan in the INL near a labeled ganglion cell, 5 days after contralateral V1 injection, shows only GFP-labeled amacrine cells and no Müller cells. The position of the ganglion-cell body in the GCL is indicated by the red circle. The scale bar represents 100 μm.

(E) Proportion of the number of Müller and amacrine cells in the INL after contralateral-eye and V1 injection at 5 days.

[4]. One explanation is that these non-ipRGC types also project to the SCN, IGL, and OPN, because at 5 days, the dLGN and the SC are not labeled (Figure 1E). An alternative explanation is that PRV spreads through gap junctions to other types of ganglion cells [24].

The PRV-infected ipRGCs could be classified into three classes based on their depth of dendritic ramification. Figure 1F shows examples of melanopsin and GFP double-stained ganglion types. Each type could be found at all eccentricities (Figure S1B). Type 1 ipRGCs (n = 66) have dendrites close to the inner nuclear layer (INL), type 2 ipRGCs (n = 69) have dendrites close to the ganglion-cell layer (GCL), and type 3 ipRGCs (n = 35) are bistratified, having dendrites in the same strata as type 1 and type 2 cells (Figure 1F).

Common Properties of Local Circuits of PRV152-Labeled Ganglion Cells

The local circuits of the PRV152-infected ganglion cells can also be labeled. PRV152 was injected into the AntC of the right eye (n = 32 retinas) as before, but, in order to mark the cells in synaptic contact with the PRV152-infected ipRGCs, we waited 5 days before dissecting the left retina. At this time, a number of other cell types in the INL became intensely GFP positive (Figure 2A). The newly infected melanopsin-negative ganglion cells were not yet surrounded by cells in the INL, suggesting that the passage of PRV from non-ipRGCs has not yet happened at this stage of infection. Most of the labeled cells in the INL were amacrine and Müller glia cells (Figure 2A). Only occasionally have we seen labeled bipolar cells. Müller-cell labeling was consistently observed solely near the cell bodies of infected ganglion cells, whereas labeled amacrine cells were scattered concentrically around them (Figure 2A). Müller cells are easily identified from confocal stacks because their processes span the entire width of the retina. Their presence was further confirmed by staining of the retina with an antibody against glutamine synthetase, a marker specific to Müller cells (Figure 2B). Double labeling with melanopsin and GFP showed that Müller cells were indeed in close proximity to ipRGCs (Figure 2C). Surprisingly, however, no Müller-cell labeling was seen in the retina when PRV152 was injected into the V1 (Figures 2D and 2E). In the INL, only the amacrine cells were GFP positive. This was true even at 5 days after injection into the V1, at a time when large numbers of ganglion and amacrine cells are labeled. These results suggest that Müller cells make specialized contacts with ipRGCs but not with ganglion cells that project to the dLGN and subsequently to the V1.

Amacrine-cell labeling is unlikely to be caused by a release of PRV particles from Müller cells, because infection of amacrine and Müller cells is temporally and

(F) GFP-labeled ipRGC subtypes in the left retina 3.5–4 days after PRV152 injection into the AntC of the right eye. Colocalization with GFP (green) and melanopsin (red) antibodies is shown. Arrows indicate soma. Side views are shown below top views and indicate dendritic stratification in the IPL between the INL and the GCL (marked by DAPI, blue). Scale bars represent 20 μm.

Please cite this article in press as: Viney et al., Local Retinal Circuits of Melanopsin- Containing Ganglion Cells Identified by Transsynaptic Viral Tracing, Current Biology (2007), doi:10.1016/j.cub.2007.04.058

spatially independent (Figure S2 and Movie S1). Further support for the idea that amacrine labeling is caused by transsynaptic release from ganglion cells comes from the finding that retinal strata juxtaposed to the GFP-positive thin strata were not labeled (Figure S3).

We find a clear difference between the number of infected amacrine and bipolar cells in the retina because very few bipolar cells become GFP-positive through PRV spread from the contralateral eye. To show that this observation in our experiments was not due to the fact that some of the labeled ganglion cells contain their own photopigments and, therefore, might lack bipolar input, we investigated retinas retrogradely labeled with PRV152 from the SC or the V1. Similar to results of tracing from the contralateral eye, very few bipolar cells were detected after SC or V1 injection (data not shown). Other studies have also shown that melanopsin-expressing ganglion cells receive synaptic input from bipolar cells [2, 3]. This suggests that PRV152 spreads across unconventional, bipolar-to-ganglion ribbon synapses with low efficiency. Interestingly, the bipolar and amacrine-cell GFP-expression levels were the same, suggesting that differential expression from the cytomegalovirus (CMV) promoter of PRV is not the cause of inefficient bipolar labeling.

Monostratified Amacrine Cells Provide Inhibitory Input to Type 2 ipRGCs

We investigated the structure and function of the local circuit of type 2 ipRGCs. For this detailed circuit tracing, we used low-titer virus injections (10^3 plaque-forming units [PFUs]) that yielded sparse circuit labeling to avoid confusion of circuits belonging to neighboring ganglion cells. These ganglion cells have dendrites in the IPL close to the ganglion-cell layer at 30% (±4%, n = 57) depth. We made 3D reconstructions of the processes of amacrines that surrounded type 2 ipRGCs (Figures 3A–3C, Movie S2). For amacrine cells that were farther away from the labeled ganglion cells, we made a number of overlapping confocal stacks and stitched them together (Figures 3D and 3E). All labeled amacrine cells studied this way (n = 20), independent of their distance from the ganglion-cell body, were monostratified in the same stratum as the type 2 ipRGCs. Although the GFP labeling of bipolar cells was rare [2, 3], in some cases (n = 3) we could reconstruct their morphology. As expected, these bipolar cells costratified with type 2 ipRGC dendrites (Figure 3F). The structure of a type 2 ipRGC local circuit, based on the detailed confocal reconstructions, is summarized in a circuit drawing in Figure 3G. The local circuit consists of three cell types: a type 2 ipRGC, a type 8 bipolar cell (based on [26]), and a monostratified amacrine cell. In this detailed morphological study, we could not use melanopsin colabeling because the GFP-labeled fine amacrine dendrites were only visible with rabbit anti-GFP, which was from the same species as the melanopsin antibody. We relied on the finding that at 5 days, non-ipRGCs were newly infected (were not present at 4 days); therefore, the spread of the virus to amacrines most probably had not yet happened. This is supported by the finding that non-ipRGCs were not surrounded by amacrine cells at 5 days (see above).

To show more direct evidence that the identified monostratified amacrine cells are indeed connected to ipRGCs, we isolated the retina at 3.5–4 days, at the time when 99% of the labeled ganglion cells are melanopsin positive. We determined the retinal coordinates of many labeled ganglion cells with two-photon microscopy and superfused the retina with oxygenated Ringers solution for an additional day. In these experiments, we used a new virus strain (see Experimental Procedures) that expressed a membrane-bound GFP that more clearly labeled the dendrites and axons. One day after isolation (5 days after infection), we fixed the retina and stained the circuit with rabbit anti-GFP antibodies and analyzed the circuits at the marked coordinates. The analyzed circuits are therefore, with 99% probability, local circuits of ipRGCs. The morphology of the labeled amacrine cells was identical to those described above (Figure 3H).

The labeled circuit gave very strong predictions about the direct, amacrine-cell-mediated inhibitory input to type 2 ipRGCs. In most vertebrates (except zebrafish [27]) and in all mammalian species studied, the IPL is divided into two major regions. Strata close to the GCL (sublamina B) incorporate axon terminals of ON bipolar cells; strata close to the INL (sublamina A) embody axon terminals of OFF bipolar cells [26, 28]. Because amacrine cells receive excitation from bipolar cells, the reconstructed amacrines must receive excitation only at light ON. Most amacrines are inhibitory cells. If the type 2 ipRGCs receive inhibitory input only from the reconstructed amacrines, inhibition should arrive at light ON but not at light OFF. Inhibition at light OFF would suggest a multistratified or bistratified amacrine cell, because OFF activity should travel vertically in the IPL from sublamina A to sublamina B [29]. To test these predictions, we recorded light-evoked inhibitory currents [29] from PRV-infected, GFP-labeled, type 2 ipRGCs with the whole-cell patch clamp method in the voltage clamp configuration after 4 days of infection. As mentioned before, at that time, only ipRGCs were labeled. The resting membrane voltage was −58 mV ± 4 mV (n = 8). Inhibition in type 2 ganglion cells was only evoked at light ON (n = 10) when the retina was stimulated with a 1 mm diameter white spot (Figure 3I), as predicted by the structure of the PRV-labeled local-circuit elements. This finding is in strong contrast with inhibitory currents evoked in most other ON ganglion cells in the mammalian retina (Figure 3J); in the rabbit retina, only one type of ON ganglion cell receives inhibition only at light ON. These results suggest that type 2 ipRGCs receive a strong, fast inhibitory input at light onset from a single morphological type of amacrine cell.

Dopaminergic Interplexiform Cells Are Synaptically Connected to Type 1 ipRGCs

Similar to type 2 ipRGCs, type 1 ipRGCs were surrounded by GFP-positive amacrine cells (Figure 4A). These amacrine cells had processes in the same strata as type 1 ipRGCs. Because the morphology and stratification of the labeled INL cells were very similar to those of a well-described cell subtype, the dopaminergic interplexiform/amacrine cells [30], we triple-labeled retinas for tyrosine hydroxylase (TH), GFP, and melanopsin. Figures 4B–4E show that a number of amacrine cells around a melanopsin- and GFP-positive type 1 ipRGC (Figure 4E) were both GFP and TH positive. Figures 4C and 4D show that TH-positive processes and

Please cite this article in press as: Viney et al., Local Retinal Circuits of Melanopsin- Containing Ganglion Cells Identified by Transsynaptic Viral Tracing, Current Biology (2007), doi:10.1016/j.cub.2007.04.058

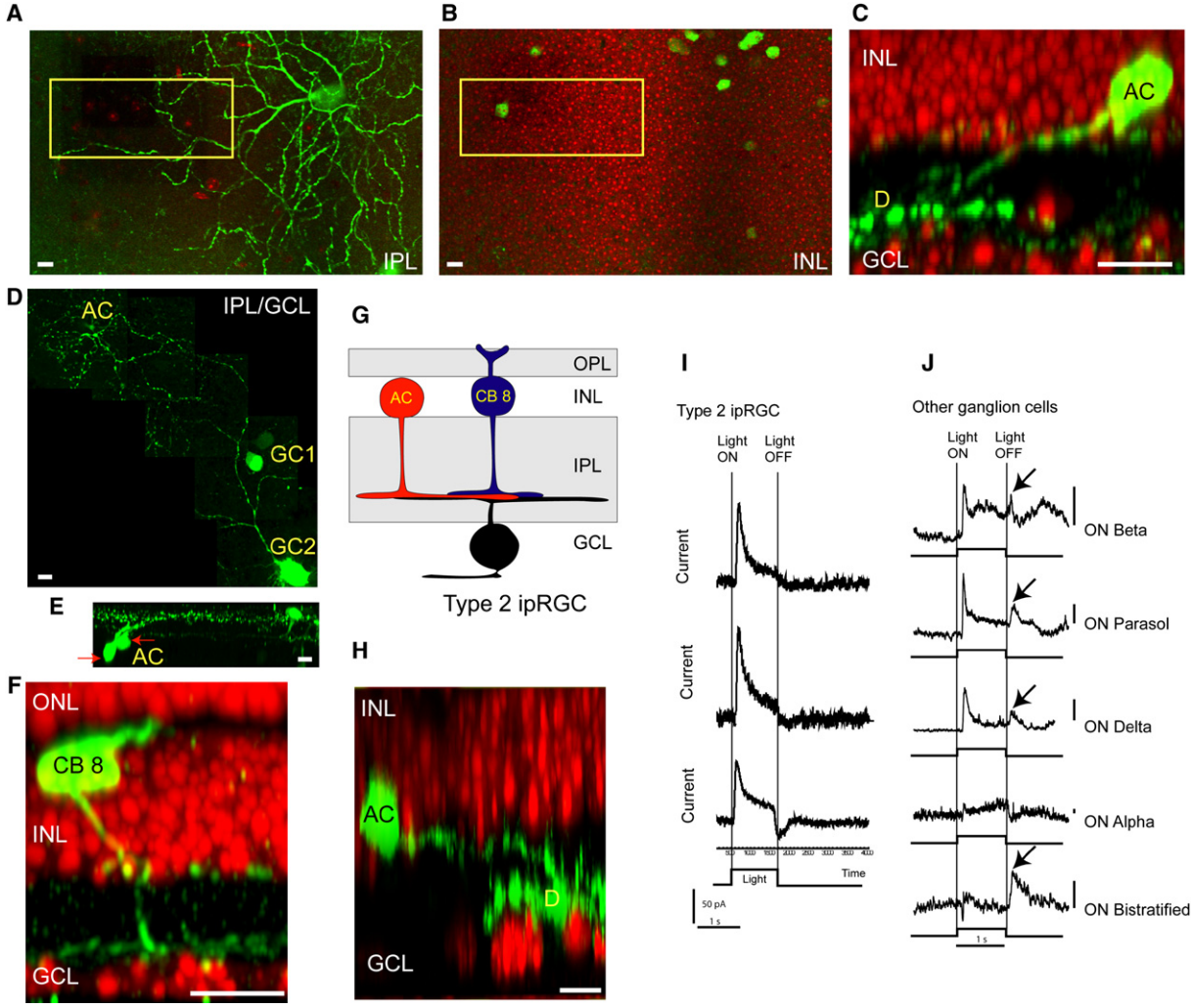

Figure 3. Local Circuit and Physiology of Type 2 ipRGCs

(A) Confocal scan in the proximal part of the IPL in the left retina at 5 days after PRV152 injection into the right eye. A GFP-labeled (green) type 2 ipRGC is shown.

(B) Confocal scan of the same area as in (A) but in the INL. The GFP-labeled cells are amacrine cells. Cell nuclei labeled by DAPI are shown in red.

(C) An x-z projection of a high-resolution scan of the yellow box shown in (A) and (B). An amacrine cell (AC) in contact with the dendrites (indicated by "D") of the type 2 ipRGC is shown. The 3D confocal scan is shown in Movie S2.

(D) Five confocal scans were stitched together to show the dendritic arbor of two amacrine cells (ACs) and of a type 2 ipRGC (GC2). A type 1 ipRGC is also shown (GC1), although its dendrites are not visible because they are in a different depth.

(E) An x-z projection of the stack shown in (D). Here the dendrites of the two amacrines, as well as the type 1 ipRGC, are shown. Red arrows point to the two amacrine cell bodies.

(F) An x-z projection of a high-resolution scan from another type 2 ipRGC shows a type 8 cone bipolar cell (CB 8).

(G) The identified cell types, based on the viral tracing, in the local circuit of type 2 ipRGCs.

(H) The same as (C), except that this amacrine cell was from an experiment where the retina was isolated at 4 days and kept in a perfusion chamber for 1 day (see main text). Scale bars represent 10 μm for all figures.

(I) Light-evoked inhibitory currents from three different type 2 ipRGCs. Inhibition cannot be detected after light OFF. The currents were measured in voltage clamp at 0mV holding potential [29]. The stimulus was a 1-mm-diameter bright spot. The timing of the stimulus is indicated by black bars.

(J) Light-evoked inhibitory currents from five different types of ON ganglion cells in the rabbit retina. Light evokes inhibition at both light ON and light OFF in four out of the five cell types (names shown to the right of each). The OFF response is indicated by arrows. The stimulus is the same as in (A). Scale bars represent 100 pA.

melanopsin-positive dendrites of ipRGCs cofasciculate in the IPL. These results suggest that dopaminergic cells provide synaptic input to type 1 cells.

Dopaminergic amacrine cells in the mouse retina are interplexiform cells that have processes in the IPL and in the outer plexiform layer (OPL) [30–33]. Five and a half to six days after contralateral virus infection, a number of horizontal cells become labeled with GFP (Figure 4F). The PRV labeling of horizontal cells suggests that these cells are not only postsynaptic targets [34] of but also presynaptic to dopaminergic interplexiform cells. Our previous finding that PRV152 very inefficiently passes to bipolar cells and the fact that no bipolar cells were detected in the vicinity of the labeled horizontal cells (data not shown) indicate that the virus spread from interplexiform cells to horizontal cells.

Please cite this article in press as: Viney et al., Local Retinal Circuits of Melanopsin- Containing Ganglion Cells Identified by Transsynaptic Viral Tracing, Current Biology (2007), doi:10.1016/j.cub.2007.04.058

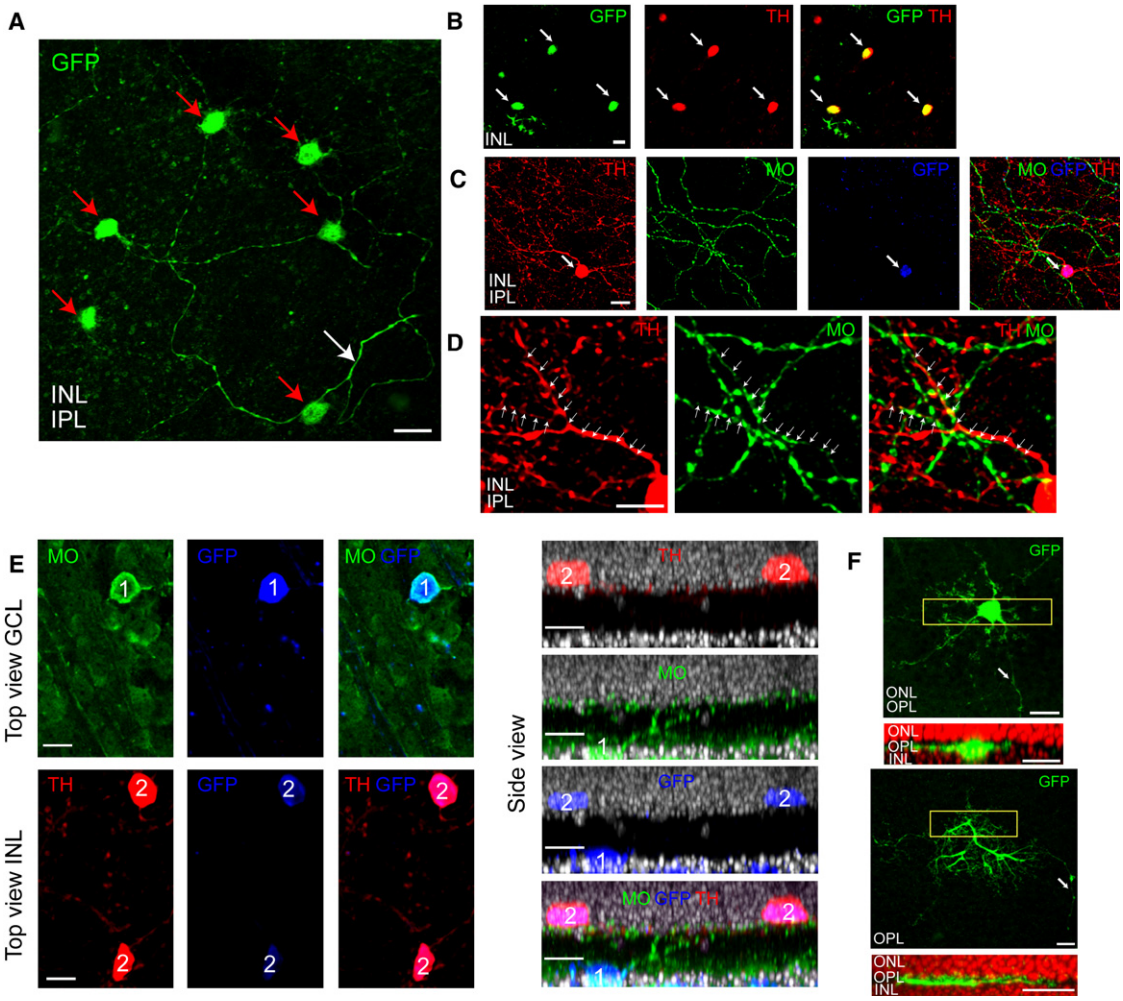

Figure 4. Type 1 ipRGCs Are Synaptically Connected to Dopaminergic Amacrine/Interplexiform Cells

(A) Confocal scan of a region in the INL–IPL border around a GFP-positive type 1 ipRGC. A descending dendrite of the ipRGC is shown by the white arrow. Red arrows point to a number of GFP-positive cell bodies in the INL.

(B) Colocalization of GFP (green) and TH (red) in amacrine cells around a type 1 ipRGC in the INL. Arrows point to double-labeled cells.

(C) Triple staining for TH (red), melanopsin (green), and GFP (blue) at the IPL–INL border. The arrow points to the TH- and GFP-positive amacrine cell.

(D) Higher magnification of a region in (C). Arrows point to cofasciculating TH- and melanopsin-positive processes.

(E) Triple staining for TH (red), melanopsin (green), and GFP (blue) labels a type 1 ipRGC (cell labeled as "1") and two dopaminergic amacrines (two cells labeled as "2") in close proximity. Top views are on the left and side views are on the right.

(F) Top: A confocal scan of a region in the IPL–ONL border shows a labeled horizontal cell body (left) and axon terminal (right). Bottom: A Z axis view of the yellow-window region from the upper panels.

Scale bars represent 15 μm for all panels.

Interestingly, even after 7 days of infection, we could not detect rods or cones; this reinforced our conclusion that PRV152 very inefficiently crosses ribbon synapses.

Dopamine is a neurotransmitter that is in the retina and controls light adaptation [35]. Dopaminergic cells of the mouse retina are GABAergic [30]. These cells make conventional synapses and also release neurotransmitters extrasynaptically [35–37]. Our study suggests that dopaminergic cells are in synaptic contact with type 1 ipRGCs. The synapse between dopaminergic cells and ipRGCs are GABAergic, dopaminergic, or both. It is possible that, similar to the synapse between dopaminergic cells and AII amacrine cells [37], both GABA and dopamine are released, but the postsynaptic receptors are positioned at different distances from the release site. In either case, however, the synaptic contact between interplexiform cells and ipRGCs suggests that the activity of dopaminergic cells synaptically influences the activity of and/or gene expression in ipRGCs.

Recent studies suggested that the dopaminergic system, which controls light–dark adaptation, strongly influences the circadian rhythm [38–42]. Our results suggest a circuitry link between light–dark adaptation and ipRGC function.

Supplemental Data

Experimental Procedures, three figures, and two movies are available at http://www.current-biology.com/cgi/content/full/17/11/■■■/DC1/.

Please cite this article in press as: Viney et al., Local Retinal Circuits of Melanopsin- Containing Ganglion Cells Identified by Transsynaptic Viral Tracing, Current Biology (2007), doi:10.1016/j.cub.2007.04.058

Acknowledgments

We are grateful for the assistance of Z. Springer and B. Gross Scherf. We thank F. Albeanu for his advice on building the two-photon microscope, F. Engert for providing us with the imaging software Tango, and P. Caroni for his comments on the paper. This study was supported by Office of Naval Research Multidisciplinary University Research Initiative [ONR MURI] and Naval International Cooperative Opportunities in Science and Technology Program [NICOP] grants, a Marie Curie Excellence Grant, a Human Frontier Science Program [HFSP] Young Investigator grant, and Friedrich Miescher Institute funds to B.R. I. Provencio kindly provided the melanopsin antibody. B.W. Banfield kindly provided PRV 614. Viral infections, electrophysiological recordings, and immunohistochemistry have been done at both Harvard and the Friedrich Miescher Institute. Two-photon time-lapse imaging, automatic confocal scanning, and automated image analysis were done at the Friedrich Miescher Institute. Membrane-bound-GFP-expressing PRV was developed at University of Szeged.

Received: January 11, 2007
Revised: April 28, 2007
Accepted: April 30, 2007
Published online: May 24, 2007

References

1. Fu, Y., Liao, H.W., Do, M.T., and Yau, K.W. (2005). Non-image-forming ocular photoreception in vertebrates. Curr. Opin. Neurobiol. *15*, 415–422.
2. Belenky, M.A., Smeraski, C.A., Provencio, I., Sollars, P.J., and Pickard, G.E. (2003). Melanopsin retinal ganglion cells receive bipolar and amacrine cell synapses. J. Comp. Neurol. *460*, 380–393.
3. Dacey, D.M., Liao, H.W., Peterson, B.B., Robinson, F.R., Smith, V.C., Pokorny, J., Yau, K.W., and Gamlin, P.D. (2005). Melanopsin-expressing ganglion cells in primate retina signal colour and irradiance and project to the LGN. Nature *433*, 749–754.
4. Sollars, P.J., Smeraski, C.A., Kaufman, J.D., Ogilvie, M.D., Provencio, I., and Pickard, G.E. (2003). Melanopsin and non-melanopsin expressing retinal ganglion cells innervate the hypothalamic suprachiasmatic nucleus. Vis. Neurosci. *20*, 601–610.
5. Card, J.P. (2000). Pseudorabies virus and the functional architecture of the circadian timing system. J. Biol. Rhythms *15*, 453–461.
6. Jons, A., and Mettenleiter, T.C. (1997). Green fluorescent protein expressed by recombinant pseudorabies virus as an in vivo marker for viral replication. J. Virol. Methods *66*, 283–292.
7. Smith, B.N., Banfield, B.W., Smeraski, C.A., Wilcox, C.L., Dudek, F.E., Enquist, L.W., and Pickard, G.E. (2000). Pseudorabies virus expressing enhanced green fluorescent protein: A tool for in vitro electrophysiological analysis of transsynaptically labeled neurons in identified central nervous system circuits. Proc. Natl. Acad. Sci. USA *97*, 9264–9269.
8. Boldogkoi, Z., Erdelyi, F., Sik, A., Freund, T.F., and Fodor, I. (1999). Construction of a recombinant herpesvirus expressing the jellyfish green fluorescent protein. Luminescence *14*, 69–74.
9. Boldogkoi, Z., Reichart, A., Toth, I.E., Sik, A., Erdelyi, F., Medveczky, I., Llorens-Cortes, C., Palkovits, M., and Lenkei, Z. (2002). Construction of recombinant pseudorabies viruses optimized for labeling and neurochemical characterization of neural circuitry. Brain Res. Mol. Brain Res. *109*, 105–118.
10. Yoon, H., Enquist, L.W., and Dulac, C. (2005). Olfactory inputs to hypothalamic neurons controlling reproduction and fertility. Cell *123*, 669–682.
11. DeFalco, J., Tomishima, M., Liu, H., Zhao, C., Cai, X., Marth, J.D., Enquist, L., and Friedman, J.M. (2001). Virus-assisted mapping of neural inputs to a feeding center in the hypothalamus. Science *291*, 2608–2613.
12. Pomeranz, L.E., Reynolds, A.E., and Hengartner, C.J. (2005). Molecular biology of pseudorabies virus: Impact on neurovirology and veterinary medicine. Microbiol. Mol. Biol. Rev. *69*, 462–500.
13. Pickard, G.E., Smeraski, C.A., Tomlinson, C.C., Banfield, B.W., Kaufman, J., Wilcox, C.L., Enquist, L.W., and Sollars, P.J. (2002). Intravitreal injection of the attenuated pseudorabies virus PRV Bartha results in infection of the hamster suprachiasmatic nucleus only by retrograde transsynaptic transport via autonomic circuits. J. Neurosci. *22*, 2701–2710.
14. Smeraski, C.A., Sollars, P.J., Ogilvie, M.D., Enquist, L.W., and Pickard, G.E. (2004). Suprachiasmatic nucleus input to autonomic circuits identified by retrograde transsynaptic transport of pseudorabies virus from the eye. J. Comp. Neurol. *471*, 298–313.
15. Coombs, J., van der List, D., Wang, G.Y., and Chalupa, L.M. (2006). Morphological properties of mouse retinal ganglion cells. Neuroscience *140*, 123–136. Published online June 19, 2006. 10.1016/j.neuroscience.2006.02.079.
16. Sun, W., Li, N., and He, S. (2002). Large-scale morphological survey of mouse retinal ganglion cells. J. Comp. Neurol. *451*, 115–126.
17. Kong, J.H., Fish, D.R., Rockhill, R.L., and Masland, R.H. (2005). Diversity of ganglion cells in the mouse retina: Unsupervised morphological classification and its limits. J. Comp. Neurol. *489*, 293–310.
18. Masland, R.H. (2001). The fundamental plan of the retina. Nat. Neurosci. *4*, 877–886.
19. Wassle, H. (2004). Parallel processing in the mammalian retina. Nat. Rev. Neurosci. *5*, 747–757.
20. Haverkamp, S., and Wässle, H. (2000). Immunocytochemical analysis of the mouse retina. J. Comp. Neurol. *424*, 1–23.
21. Card, J.P., Whealy, M.E., Robbins, A.K., Moore, R.Y., and Enquist, L.W. (1991). Two alpha-herpesvirus strains are transported differentially in the rodent visual system. Neuron *6*, 957–969.
22. Hattar, S., Kumar, M., Park, A., Tong, P., Tung, J., Yau, K.W., and Berson, D.M. (2006). Central projections of melanopsin-expressing retinal ganglion cells in the mouse. J. Comp. Neurol. *497*, 326–349.
23. Hannibal, J., and Fahrenkrug, J. (2004). Target areas innervated by PACAP-immunoreactive retinal ganglion cells. Cell Tissue Res. *316*, 99–113.
24. Sekaran, S., Foster, R.G., Lucas, R.J., and Hankins, M.W. (2003). Calcium imaging reveals a network of intrinsically light-sensitive inner-retinal neurons. Curr. Biol. *13*, 1290–1298.
25. Hattar, S., Liao, H.W., Takao, M., Berson, D.M., and Yau, K.W. (2002). Melanopsin-containing retinal ganglion cells: Architecture, projections, and intrinsic photosensitivity. Science *295*, 1065–1070.
26. Ghosh, K.K., Bujan, S., Haverkamp, S., Feigenspan, A., and Wässle, H. (2004). Types of bipolar cells in the mouse retina. J. Comp. Neurol. *469*, 70–82.
27. Connaughton, V.P., Graham, D., and Nelson, R. (2004). Identification and morphological classification of horizontal, bipolar, and amacrine cells within the zebrafish retina. J. Comp. Neurol. *477*, 371–385.
28. Famiglietti, E.V., Jr., and Kolb, H. (1976). Structural basis for ON-and OFF-center responses in retinal ganglion cells. Science *194*, 193–195.
29. Roska, B., and Werblin, F. (2001). Vertical interactions across ten parallel, stacked representations in the mammalian retina. Nature *410*, 583–587.
30. Gustincich, S., Feigenspan, A., Wu, D.K., Koopman, L.J., and Raviola, E. (1997). Control of dopamine release in the retina: A transgenic approach to neural networks. Neuron *18*, 723–736.
31. Dowling, J.E., and Ehinger, B. (1975). Synaptic organization of the amine-containing interplexiform cells of the goldfish and Cebus monkey retinas. Science *188*, 270–273.
32. Marc, R.E., and Liu, W.L. (1984). Horizontal cell synapses onto glycine-accumulating interplexiform cells. Nature *312*, 266–269.
33. Mangel, S.C., and Dowling, J.E. (1985). Responsiveness and receptive field size of carp horizontal cells are reduced by prolonged darkness and dopamine. Science *229*, 1107–1109.
34. Lasater, E.M., and Dowling, J.E. (1985). Dopamine decreases conductance of the electrical junctions between cultured retinal horizontal cells. Proc. Natl. Acad. Sci. USA *82*, 3025–3029.

35. Witkovsky, P. (2004). Dopamine and retinal function. Doc. Ophthalmol. *108*, 17–40.
36. Puopolo, M., Hochstetler, S.E., Gustincich, S., Wightman, R.M., and Raviola, E. (2001). Extrasynaptic release of dopamine in a retinal neuron: Activity dependence and transmitter modulation. Neuron *30*, 211–225.
37. Contini, M., and Raviola, E. (2003). GABAergic synapses made by a retinal dopaminergic neuron. Proc. Natl. Acad. Sci. USA *100*, 1358–1363.
38. Sakamoto, K., Liu, C., Kasamatsu, M., Pozdeyev, N.V., Iuvone, P.M., and Tosini, G. (2005). Dopamine regulates melanopsin mRNA expression in intrinsically photosensitive retinal ganglion cells. Eur. J. Neurosci. *22*, 3129–3136.
39. Sakamoto, K., Liu, C., and Tosini, G. (2004). Classical photoreceptors regulate melanopsin mRNA levels in the rat retina. J. Neurosci. *24*, 9693–9697.
40. Doi, M., Yujnovsky, I., Hirayama, J., Malerba, M., Tirotta, E., Sassone-Corsi, P., and Borrelli, E. (2006). Impaired light masking in dopamine D2 receptor-null mice. Nat. Neurosci. *9*, 732–734.
41. Steenhard, B.M., and Besharse, J.C. (2000). Phase shifting the retinal circadian clock: xPer2 mRNA induction by light and dopamine. J. Neurosci. *20*, 8572–8577.
42. Hannibal, J., Hindersson, P., Knudsen, S.M., Georg, B., and Fahrenkrug, J. (2002). The photopigment melanopsin is exclusively present in pituitary adenylate cyclase-activating polypeptide-containing retinal ganglion cells of the retinohypothalamic tract. J. Neurosci. *22*, RC191.
43. Franklin, K., and Paxinos, G. (1997). The Mouse Brain in Stereotaxic Coordinates. (San Diego, California: Academic Press).